2018 26th Mediterranean Conference on Control and Automation (MED)
Zadar, Croatia, June 19-22, 2018

Reactive Control Technology for 3D Navigation of Nonholonomic Robots in Tunnel-Like Environments Based on Limited Sensory Data*

Alexey S. Matveev[1], Valentin V. Magerkin[1], and Andrey V. Savkin[2]

Abstract— **A constant-speed nonholonomic robot should pass through an unstructured and unknown 3D tunnel-like cave environment. The sensors provide information about the nearest point of tunnel's surface and the distance to the surface along any ray going from the robot at an upper-limited angle with respect to the direction toward the nearest point. A new navigation law is presented that solves the mission, respects a given safety margin to the surface, drives the robot to the pre-specified distance to it, and then maintains this distance. This law generates the control as a reflex-like reaction to the current observation. Mathematically rigorous justification of this law is provided; its applicability is confirmed by computer simulation tests.**

I. Introduction

Many recent and emerging applications of mobile robotics involve the task of autonomously traveling in 3D through an unknown and unstructured tunnel-like cave environment. Examples include, but are not limited to, search and rescue operations in marine wreckage sites [1], indoor and city exploration, rescue, and surveillance operations by means of micro air vehicles (MAV's) [2], inspection of offshore installations, underwater archeology and environmental studies [3]–[5], as well as inspection and service of storm runoff networks, channelized aquifers, mines, bypass tunnels for dams, freshwater delivery tunnels, pipelines in sewer networks, power plants, factories, petrochemical, water supply and fluid transportation industries [6]–[8].

For many such missions, aerial and underwater robotics are viewed as holding promise of emerging technology with a higher level of flexibility and efficacy. To acquire these benefits, the robots should be able to operate safely and autonomously through long time and distance scales. Safety means, at least, that the robot should not collide with the tunnel wall. Subject to this limitation, the robot is free to move in all three dimensions. This brings challenge of 3D navigation in an unknown narrow environment; at the minimum, high computations expense of the navigation algorithm has been a usual price for resolution of this challenge.

Meanwhile, the main focus was on in-pipe inspection and service robots up to now. They usually operate in contact with the tunnel boundary surface [6], [8]. This may facilitate directional navigation inside a narrow pipe, e.g., the very deployment of some robots in a straight pipe settles their orientation and, thus, direction of motion. Local behavior control of such robots usually benefit from a rather full and omni-directional sensory awareness about the surroundings. Solution of global navigation tasks is aided by the fact that the workspace is typically structured and assembled of finitely many primitives (straight pipe, crossroad, T-junction, dead-end, etc.), whereas their parameters (e.g., diameters) or even a map of a pipeline may be known a priori.

This paper deals with another situation: 3D tunnel-like cave environment is unstructured, unknown, and not necessarily "narrow"; local geometric properties of the tunnel boundary surface are not anyhow restricted. Perception of the robot is confined to a close small patch of this surface; the "opposite patch" may be out off the sensing distance.

Without an exterior assistance, such overhead and confined environments still represent a real challenge for underwater autonomous navigation, and most pertinent missions are still carried out by human divers or remotely teleoperated vehicles up to now [3], [5]; some robotic experiments in flooded natural cenotes are yet reported in [9].

For navigation of MAV's in most indoor and many confined urban environments, typical troubles arise from the lack of access to GPS and drift-over-time deterioration of dead-reckoning positioning. Typical approaches to such navigation [10] feature various limitations, like reliance on known landmarks, salient features or environmental patterns [11], maps, a priori image-databases [12], local positioning systems [13], or a partially structured environment [14]. Some of these methods, including simultaneous 3D localization and mapping (SLAM), are computationally expensive, are hardly implementable on-board, and so employ off-board computations [2], which calls for highly reliable communication and may cause harmful feedback delays.

Meanwhile, there is an ever-growing interest to solution of navigation tasks by means of a simpler and cheaper hardware, and at a lower computational cost. This challenges the classic paradigm of splitting the algorithm into path planning and path tracking. *Is it feasible to fuse them into a single, computationally cheap rule or, more pragmatically, to which extent, under which circumstances, and how rules of such kind can cope with robot navigation through a tunnel?*

This paper provides evidence that autonomous long-distance advancement through a generic tunnel can be accomplished, on certain occasions, at a minor computational cost: control signal is a reflex-like reaction to the current observation. This is feasible in spite of ordinary limitations of robot's hardware (such as finite control range, under-

*This work was supported by the Australian Research Council, and by the Russian Science Foundation, project 14-21-00041p.

[1]A.S. Matveev and V.V. Magerkin are is with the Department of Mathematics and Mechanics, Saint Petersburg University, 198905, St. Petersburg, Russia almat1712@yahoo.com, magerkin93@gmail.com

[2]A.V. Savkin is with the School of Electrical Engineering and Telecommunications, the University of New South Wales, Sydney, 2052, NSW, Australia a.savkin@unsw.edu.au

actuation, nonholonomy, poor knowledge of the scene, limited sensory capacity). In parallel with passing through the tunnel, approaching its surface and subsequently maintaining a pre-specified distance to it can also be arranged.

To this end, we examine a robot that travels in 3D with a constant speed and is actuated by the acceleration vector, which is upper bounded in norm and is perpendicular to the velocity to keep the speed constant. This model mainly applies to constant-speed vehicles propelled in the surge direction and driven by the yawing and pitching rates, but also covers some other cases [15].

The robot operates inside a tunnel, with the main objective to progress through it. In a nutshell, "tunnel" is viewed as a 3D cave-like workspace for which a fully informed external observer is able to identify a current "direction of advancement along the tunnel" at any its point. Meanwhile, the robot has access only to a small patch of tunnel's boundary S: it determines the direction to the closest point of S and the distance to S along any ray outgoing from the robot at an upper-limited angle with respect to this direction.

We first disclose a trade-off between the contortion of the tunnel and the turning capacity of the robot necessary for feasibility of the mission; the assumptions of our theoretical analysis are slight and partly inevitable enhancement of these. We also discuss geometric features of the tunnel that enable global navigation through it based on observing only local nearby patches of its boundary. A reactive navigation law is then presented that solves the mission, drives the robot to a pre-specified "comfortable" distance to the tunnel wall, stably maintains this distance afterwards, and always respects a given safety margin to this wall. Mathematically rigorous justification of this law is provided; its applicability and performance are confirmed by computer simulation tests.

This paper develops some ideas from [15]–[20]. The kinematic model is borrowed from [15], [20]. The papers [16], [17] deal with 2D workspaces, whereas [15] and [20] handle different navigation problems in 3D-space (seeking an extremum of a scalar field and scanning the whole of a 2D surface, respectively) so that their findings are critically insufficient to solve the problem considered in this paper.

Its body is organized as follows. Sections II and III give a preliminary and final setup of the problem, respectively. Section IV is devoted to necessary conditions for the mission solvability and assumptions of theoretical analysis. Section V discusses a particular way of access to local features of tunnel's surface that are used for navigation. The control law and the main results are presented in Sections VI and VII, respectively. Section VIII reports on computer simulation tests. Due to the page limit, the proofs of the stated results will be given in the full version of the paper.

Throughout the paper, the following notations are used:

- $\langle A;B\rangle$ and $A\times B$, inner and cross product;
- $\|\cdot\|$, Euclidean norm of a vector and spectral norm of a matrix and linear operator;
- $\pi(r)$, set of all *projections* of point $r\in\mathbb{R}^3$ onto the surface $S\subset\mathbb{R}^3$, i.e., points $s\in S$ such that

$$\|r-s\|=\mathbf{d}_S[r]:=\min_{s'\in S}\|s'-r\|. \tag{1.1}$$

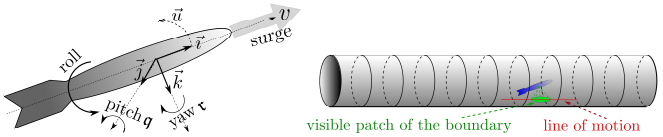

(a) (b)

Fig. 1. (a) A vehicle in 3D; (b) Extracting the correct line of motion.

II. The System and Fuzzy Setup of the Problem

We consider a nonholonomic robot that moves in the 3D-space $\mathbb{R}^3$ with a constant surge speed v and is actuated by bounded pitching and yawing rates; see Fig. 1(a). Like in [15], we ignore the roll motion of the robot and use the abridged classic kinematic model of the 3D unicycle:

$$\dot r=v\vec\imath,\quad \dot{\vec\imath}=\vec u\in\mathbb{R}^3,\quad \langle\vec u;\vec\imath\rangle=0,\quad \|\vec u\|\le\overline{u}. \tag{2.2}$$

Here $r\in\mathbb{R}^3$ is the location of the robot, $\vec\imath$ is the unit vector along its centerline, $\vec u$ is the control input, and $\overline{u}>0$ is given. The third equation in (2.2) keeps $\|\vec\imath\|\equiv 1$. Overall, the model (2.2) captures that the robot's speed is constantly v and the robot travels over space paths whose curvature radius $\ge v/\overline{u}$.

The control $\vec u$ can be replaced by the pitching $\mathfrak{q}$ and yawing $\mathfrak{r}$ rates due to a one-to-one correspondence $\vec u\leftrightarrow(\mathfrak{q},\mathfrak{r})$ [15, Rem. 2.1]. The model (2.2) also applies to many mechanical systems that can move not only in the surge direction [15].

The robot operates in a tunnel-like workspace bounded by a surface $S\subset\mathbb{R}^3$ and should respect a given distance margin $d_{\text{safe}}>0$ to S. It is required to design a control law that ensures constant progress of the robot through the tunnel, possibly after a transient period. If the time of operation is large enough, a certain "comfortable" value d_* of the distance to S should be eventually approached and then maintained.

In its local frame, the robot identifies the direction $\vec d$ toward the closest point $\pi(r)$ of S and also measures the distance to S along any ray emitted from r at an angle $\le\alpha_s$ to $\vec d$, where $\alpha_s>0$ is given. So the robot "sees" only a small nearby patch of S around $\pi(r)$ and has to infer the direction of "advancing through the tunnel" from these local data.

Hence the mission is possible not for any S: at least, "advancement through the tunnel" must be of sense and its direction must be recognizable from the sensed small patches of S. Such a case is exemplified by the right circular cylinder in Fig. 1(b): the above direction is given by the generatrix and can be found as that in which any patch of S has zero curvature. Inspired by this sample, we will deal with surfaces whose signed curvature is minimal in an acceptable direction of motion. The purpose of the next section is to flesh out this.

III. Rigorous Setup of the Problem

We start with rigorous definition of the class of surfaces S to be dealt with. Let $\mathbb{B}$ be either a) the real line $\mathbb{R}$, or b) the unit circle $S^1\subset\mathbb{R}^2$, or c) a finite interval $[b_-,b_+]\subset\mathbb{R}$.

Definition 3.1: A *tunnel with the basis* $\mathbb{B}$ and *projection* $B: S \to \mathbb{B}$ is a C^3-smooth regular surface S (with the one-dimensional boundary $\partial S = B^{-1}[b_-] \cup B^{-1}[b_+]$ in the case c)) such that the following statements hold: **i)** The projection is C^3-smooth, maps S onto $\mathbb{B}$, its differential has rank 1 everywhere, and the inverse image of any compact subset of $\mathbb{B}$ is compact; **ii)** any *meridian* $\mathcal{M}(b) := B^{-1}[b]$ is a simple closed curve; **iii)** The set S is closed.

If $\mathbb{B} = [b_-, b_+]$, the tunnel is said to be *open*, and *closed* otherwise. Progression of robot r through the tunnel is associated with evolution of the (multivalued in general) *basic coordinate* $b(r) := \{B(s) : s \in \pi(r)\}$ in a fixed direction. The basis $\mathbb{B} = \mathbb{R}$ is used to model a "very long tunnel". The basis $\mathbb{B} = S^1$ addresses missions where the robot has to circulate through a cavity homeomorphic to a torus.

For the cylinder $\mathcal{C}$ in Fig. 1(b), b is the coordinate along the axis of symmetry and the meridians are the perpendicular sections. This tunnel is open and ∂S consists of the two extreme meridians. Extending $\mathcal{C}$ to the left and right without limits gives a closed infinite tunnel. Another example is the surface obtained via revolving the graph Γ of a function $f(\cdot) > 0$ defined on the axis of revolution *AoR*; the meridians are the paths of the points of Γ, and b is the coordinate along *AoR*. A closed compact tunnel is exemplified by any torus, which is obtained by revolving a circle about a coplanar axis. Then the meridians are the snapshots of the moving circle and $b = (\cos\varphi, \sin\varphi) \in S^1$ assesses the rotation angle φ. Any diffeomorphism J of an open vicinity of a tunnel S onto an open subset of $\mathbb{R}^3$ transforms S to a new tunnel.

For an open tunnel, the robot should reach its *end*, i.e., $\pi(r)$ must arrive at the δ_s-vicinity of ∂S, where $\delta_s > 0$ is given. We assume that the robot can recognize the end from the sensory data. For a closed tunnel, the coordinate b should eventually evolve in an unaltered direction. The following definition comprises these considerations.

Definition 3.2: The robot is said to *solve the tunnel* if

$$d(t) := \mathbf{d}_S[r(t)] = \|\vec{d}(t)\| \geq d_{\text{safe}} > 0 \quad \forall t \tag{3.1}$$

and there exists time t_0 such that

- If the tunnel is open, $\pi[r(t_0)]$ is in the δ_s-vicinity of ∂S;
- Otherwise, the following statements are true for $t \geq t_0$:
  - **i)** Robot's basic coordinate $b(t)$ is unique, smoothly depends on time, and $\pm\dot{b}(t) \geq \eta$, where the sign in $\pm$ and $\eta > 0$ do not alter with time;
  - **ii)** In (3.1), $d(t)$ monotonically tends to d_* as $t \to \infty$.

If $\mathbb{B} = S^1$, the derivative $\dot{b}$ is viewed as that of the angular coordinate of $b \in S^1$. For the sake of definiteness, we assume that the robot operates inside the tunnel.

In what follows, we use the following notations:

- $\mathfrak{T}_s(S)$, plane tangent to S at $s \in S$;
- $N(s)$, unit normal to S directed inside the tunnel;
- $D_V W$, derivative of the field W in direction of V;
- $\mathcal{S}_s(V) = -D_V N$, shape operator (Weingarten map);
- $\mathbf{II}_s[V;W] := \langle \mathcal{S}_s(V); W \rangle, V, W \in \mathfrak{T}_s(S)$, second fundamental form (shape tensor);
- $\varkappa_-(s) \leq \varkappa_+(s)$, principal curvatures, i.e., the eigenvalues of the quadratic form $\mathbf{II}_s[\cdot;\cdot]$;
- $E_\pm(s)$, respective unit eigenvectors (principal eigenvectors) continuously depending on $s \in S$;
- $p_\pm(s)$, lines spanned by $E_\pm(s)$ (principal directions);
- $\vec{\tau}(s) \in \mathfrak{T}_s(S)$, smooth unit vector-field tangent to the meridian $\mathcal{M}[b(s)]$ that passes through s;
- $\vec{\tau}_*(s_*) \in \mathfrak{T}_{s_*}[S(d_*)]$, similar field on $S(d_*)$, where
- $S(d_*) := \{p = s + d_* N(s), s \in S \setminus \partial S\}$, locus of the desired locations of the robot;
- $\mathbf{Pr}_L$, orthogonal projection onto a subspace $L \subset \mathbb{R}^3$.

Now we describe a class of tunnels for which the direction "along the tunnel" is recognizable from its small patches.

Definition 3.3: A tunnel is said to be *regular* if at any point $s \in S$, the signed normal curvature of S in the meridian direction $\vec{\tau}(s)$ is not minimal and, moreover, is separated from $\varkappa_-(s)$ by a gap $\Delta_\tau > 0$ that does not depend on s:

$$\mathbf{II}_s[\vec{\tau}(s); \vec{\tau}(s)] \geq \varkappa_-(s) + \Delta_\tau. \tag{3.2}$$

The second claim follows from the first one if S is compact. Since $\varkappa_-(s) < \varkappa_+(s)$ by (3.2), the principal directions $p_\pm(s)$ and vector-fields $E_\pm$ are well-defined.

The right circular cylinder from Fig. 1(b) is a regular tunnel since $\varkappa_- = 0$ (this is attained at any generatrix) and the meridian curvatures are positive. For the surface of revolution, the curvature of the meridian $\mathcal{M}(b)$ equals $f(b)^{-1}$. Since the curvature of Γ is $-f''(b)(1+[f'(b)]^2)^{-3/2}$, the concerned tunnel is regular if $(1+[f'(b)]^2)^{3/2} > -f''(b)f(b)\ \forall b$.

We assume that *the tunnel at hands is regular*.

Now we unveil a geometric sense of i) in Def. 3.2. It can be shown that the map $s \in S \mapsto J(s) := s + d_* N(s) \in S(d_*)$ is a diffeomorphism of S onto $S(d_*)$. So $B_* := B \circ J^{-1} : S(d_*) \to \mathbb{B}$ meets i),ii) of Def. 3.1. This gives rise $\mathcal{M}_*(b) = B_*^{-1}(b)$ to the meridians $\mathcal{M}_*(b) = J[\mathcal{M}(b)]$ on $S(d_*)$. Their tangents can be arranged into the smooth unit vector-field $\vec{\tau}_*$ on $S(d_*)$:

$$\vec{\tau}_*(r) := \frac{J'(s)\vec{\tau}(s)}{\|J'(s)\vec{\tau}(s)\|}, \quad \text{where } s := J^{-1}(r).$$

In Def. 3.2, i) means that while moving nearly over $S(d_*)$, the robot traverses the meridians in an unaltered direction at nonzero angles, and eventually crosses any meridian that lies in the direction of motion with respect to the initial one. For an open tunnel, this entails reaching its end.

IV. Assumptions of theoretical analysis

We start with disclosing conditions necessary for the robot to cope with the mission. This includes the ability to maintain the desired distance d_* to S while retaining two degrees of freedom while moving parallel to S.

Definition 4.1: The robot is said to be *locally d-controllable* at point $r \in S(d_*)$ if the directions in which it can go through r with $d \equiv d_*$ constitute a plane.

Lemma 4.1: If the robot is locally d-controllable at $r \in S(d_*)$, then the points from $\pi(r) \cup \{r\}$ are collinear and

$$1 - d_* \varkappa_+(s) > 0 \qquad \forall s \in \pi(r). \tag{4.1}$$

So the size n_r of $\pi(r)$ is at most two. If $n_r = 2$, the surface $S(d_*)$ tangentially touches itself at point r. We exclude this extraordinary case by imposing the following.

Assumption 4.1: The set $\pi(r)$ of projections of r onto S contains a single point $s(r)$ for any $r \in S(d_*)$.

Lemma 4.2: If the robot is locally d-controllable at point $r \in S(d_*)$, then for $s := s(r)$, the following holds:

$$\frac{\overline{u}}{v} \geq \max\left\{\frac{|\varkappa_-(s)|}{1-d_*\varkappa_-(s)}; \frac{|\varkappa_+(s)|}{1-d_*\varkappa_+(s)}\right\}. \tag{4.2}$$

This controllability means that whenever $d = d_*$, $\dot{d} = 0$, a proper control can set $\ddot{d} = 0$. It does not come as a surprise that if "$\geq$" is put in place of "$>$" in (4.2), the sign of $\ddot{d}$ can be freely manipulated and so the output d is locally controllable in the conventional sense. For its regulation to d_*, controllability of the output is commonly needed on the transient part of robot's path. So we enhance (4.2) via "$\geq$" $\mapsto$ "$>$" and extending local d-controlability on the entire operational zone $Z_{\rm op}$, which is defined in terms of the extreme values $d_\pm$ of d in $Z_{\rm op}$ (where $d_{\rm safe} \leq d_- < d_* < d_+$):

$$Z_{\rm op} := \{r = s + dN(s) : s \in S \setminus \partial S, d \in (d_-, d_+)\}. \tag{4.3}$$

So, ultimately, we make the following assumption.

Assumption 4.2: Assumption 4.1 and (4.1), (4.2) with "$\geq$" $\mapsto$ "$>$" are valid with any d_* from $[d_-, d_+]$. Moreover, (4.1) and (4.2) hold with a uniform gap: there exist $\Delta_\varkappa \in (0,1]$ and $\Delta_c > 0$ such that for all $d \in [d_-, d_+]$ and $s \in S$,

$$1 - d\varkappa_+(s) \geq \Delta_\varkappa, \quad \frac{\overline{u}}{v} \geq \frac{|\varkappa_\pm(s)|}{1-d\varkappa_\pm(s)} + \Delta_c. \tag{4.4}$$

The second claim follows from the first one if S is compact. In (4.4), the first inequality holds (with $\Delta_\varkappa \leq 1$) if $\varkappa_+(s) \leq 0$; otherwise, this inequality means that $1 - d_+\varkappa_+(s) \geq \Delta_\varkappa$.

To traverse the meridians in a fixed direction while moving over $S(d_*)$, the robot should block rotation of $\dot{r}$ from one side of the meridian tangent $\vec{\tau}_*$ to the other side. This claim tacitly compares mutual orientations of pairs of vectors in the case where the pairs "live" in different tangent planes along the robot's path. This is feasible thanks to the Levy-Civita connection [21, p. 442], by which the angular velocities $\omega_{\vec{\tau}_*}$ and $\omega_{\dot{r}}$ of the tangential rotation of $\vec{\tau}_*$ and $\dot{r}$, respectively, are well-defined. Thus, whenever $\dot{r}$ is aligned with $\vec{\tau}_*$, the sign of $\omega_{\dot{r}} - \omega_{\vec{\tau}_*}$ should be freely manipulable by the control input $\vec{u}$. Certainly, this should be accomplished with not violating the other control goal $d \equiv d_*$. If these do hold, the robot is said to be *locally controllable* at the posture at hands.

Lemma 4.3: Let the robot be locally controllable at any posture where $r \in S(d_*)$ and $\dot{r}$ is aligned with $\vec{\tau}_*(r)$. Then for any meridian $\mathcal{M}_*(b)$ and at any its point, $\kappa < \overline{u}/v$.

Here κ is the "own" unsigned curvature of $\mathcal{M}_*(b)$, i.e., $\kappa = \left\|\frac{d\vec{\tau}_*}{dl}\right\| = \sqrt{\kappa_n^2 + \kappa_g^2}$, where l is the arc length on the meridian, $\kappa_g = \left\|\mathbf{Pr}_{\mathfrak{T}[S(d_*)]}\frac{d\vec{\tau}_*}{dl}\right\|$ is the geodesic curvature, $\kappa_n = |\left\langle \frac{d\vec{\tau}_*}{dl}; N_* \right\rangle|$ is the normal curvature. It can be shown that the right-hand side *RHS* of (4.2) is the tight upper bound for normal curvatures of curves on $S(d_*)$. To regulate the distance d to S, the normal to $S(d_*)$ control effort $\langle \vec{u}; N_* \rangle N_*$ should be, at the worst, no less than *RHS*. It can be shown that the tangential effort $\mathbf{Pr}_{\mathfrak{T}[S(d_*)]}\vec{u}$ should be no less than κ_g to keep the angle to the meridians under control. This distribution of the control effort into normal and tangential parts depends on $S(d_*)$ and the current meridian. However, the robot has no access to these data. This motivates an universal distribution that fits any possible situation. Let $\overline{u}_N$ and $\overline{u}_\mathfrak{T}$ be the parts allocated to the normal and tangential control efforts. Then we arrive at the following.

Assumption 4.3: There exist constants $\overline{u}_N, \overline{u}_\mathfrak{T}, \Delta_\mathfrak{T} > 0$ such that $\overline{u}^2 = \overline{u}_N^2 + \overline{u}_\mathfrak{T}^2$, Assumption 4.2 holds with $\overline{u} := \overline{u}_N$, and $\overline{u}_\mathfrak{T} \geq v\kappa_g + \Delta_\mathfrak{T}$ everywhere on $S(d_*)$.

We close the section with two technical assumptions.

Assumption 4.4: The maps $N, \varkappa_\pm, E_\pm$, and ∇B are Lipschitz, i.e., there exist constants $L_N, L_\varkappa, L_E, L_B > 0$ such that

$$\begin{gathered}\|N(s_1) - N(s_2)\| \leq L_N\|s_1 - s_2\|, \\ |\varkappa_\pm(s_1) - \varkappa_\pm(s_2)| \leq L_\varkappa\|s_1 - s_2\|, \\ \|E_\pm(s_1) - E_\pm(s_2)\| \leq L_E\|s_1 - s_2\|, \\ \|\nabla B(s_1) - \nabla B(s_2)\| \leq L_B\|s_1 - s_2\| \ \forall s_1, s_2 \in S.\end{gathered} \tag{4.5}$$

The gradient $\nabla B(\cdot)$ is bounded from the both sides: there exist constants $\Delta_B^\pm > 0$ such that $\Delta_B^- \leq \|\nabla B(s)\| \leq \Delta_B^+ \ \forall s \in S$.

For a compact tunnel, this assumption necessarily holds.

To arrive at a situation where the proposed guidance system becomes locked onto S, a preliminary maneuver is performed. To this end, a unit vector $\vec{n}_{\rm in}$ perpendicular to $\vec{l}(0)$ is chosen. The maneuver is over a circular path $C_{\rm in}$ in the plane normal to $\vec{n}_{\rm in}$ and under the control signal

$$\vec{u} = \overline{u}\cdot\vec{\imath} \times \vec{n}_{\rm in}. \tag{4.6}$$

Assumption 4.5: The path $C_{\rm in}$ lies in the zone (4.3).

V. Estimator of the motion direction

Its role is to infer the direction of motion from the sensory data: the direction $\vec{d}$ from robot's location r to its projection $s := \pi(r)$ onto S and the distance $d(\alpha, \varphi)$ to S along any ray $\mathfrak{R}$ emitted from r at an angle $\alpha \in [0, \alpha_s]$ to $\vec{d}$. Here the angle φ gives the direction of $\mathfrak{R}$ in projection onto the plane $\vec{d}^\perp$ normal to $\vec{d}$. The generated direction should be transversal to the meridian passing through s to meet i) in Def. 3.2.

For example, the principal direction $p_-(s)$ might be used since it traverses the meridian due to (3.2). However, computation of $p_-(s)$ involves second-order differentiation of the sensory data, which is a highly unstable procedure. So we employ differentiation-free and simpler methods, not necessarily focused on $p_-(s)$, and adopt a whole class of them that is delineated in the following.

Definition 5.1: Motion direction estimator (MDE) maps the sensory data obtained in location r into a straight line $p(r) \subset \mathfrak{T}_{\pi(r)}(S)$ so that the map $r \in Z_{\rm op} \mapsto p(r) \in \mathbf{Gr}(1,3)$ is continuous. Its *exactness* $\beta_{\rm ex}$ is an upper bound on the angle between $p(r)$ and $p_-[\pi(r)]$ that holds for any $r \in Z_{\rm op}$.

Here $\mathbf{Gr}(1,3)$ is the Grassmanian manifold of all straight lines L in $\mathbb{R}^3$ with $L \ni 0$ [22, pp. 42-44]. The output $p(r)$ is given in the local frame of the robot. Usefulness of MDE depends on $\beta_{\rm ex}$: it should be less than the minimal angular gap between $p_-[\pi(r)]$ and the meridian tangent at $\pi(r)$ since then $p(r)$ is transversal to the meridian, as is required.

Now we discuss a particular design of DE.

Most-distant-point-based estimator (MDPBE) with parameter $\alpha_e \in (0, \alpha_s]$ finds the tangential orientations φ of the ray $\mathfrak{R}$ that furnish the local maxima of the distance $d(\alpha_e, \varphi)$, shifts every of the found φ's into $(-\pi/2, \pi/2]$ by adding, if necessary, an integer multiple of π, computes the arithmetic mean $\varphi_{\rightarrow}$ of the results, and returns the straight line p that goes in the normal plane $\vec{d}^{\perp}$ in the direction of $\varphi_{\rightarrow}$. MDPBE is well-posed if there are only finitely many local maxima.

Proposition 5.1: Let Assumptions 4.2 and 4.4 hold. For any $\beta > 0$, there is $\overline{\alpha} \in (0, \alpha_s]$ such that MDPBE is well-posed (with two local maxima) in the zone (4.3) and is a MDE with exactness β whenever $\alpha_e \in (0, \overline{\alpha})$.

Thus $\alpha_e \approx 0$ results in high exactness. Meanwhile, such an exactness is not needed: only a certain and not necessarily small upper bound (7.5) should be respected. Even arbitrarily high accuracies may be achieved with a non-small angle α_e for specific classes of tunnels. For example, it is easy to see that for the right circular cylinder from Fig. 1(b), MDPBE enjoys the absolute exactness $\beta = 0$ under any $\alpha_e \in (0, \pi/2)$.

VI. The proposed control law

This law has two discrete modes $\mathfrak{P}$ (preliminary) and $\mathfrak{M}$ (main), and switches between them in accordance with Fig. 2(a), where $\delta_{\uparrow} > 0$ is a tunable parameter. The role of $\mathfrak{P}$ is to drive the robot into an orientation nearly parallel to S. Mode $\mathfrak{M}$ directly aims at achieving the control objectives. Initially, mode $\mathfrak{P}$ is set up. At the time when $\mathfrak{P} \mapsto \mathfrak{M}$, the current distance d to S is memorized as a parameter d_{tr} to be used in the control rule; see Fig. 2(b) and (6.1).

Control rule in mode $\mathfrak{P}$ is given by (4.6).

Control rule in mode $\mathfrak{M}$ is well posed if the robot is not aligned with the direction to S, i.e., if $\vec{\imath} \times \vec{d}_0 \neq 0$ ($\Leftrightarrow \sin\psi \neq 0$), where $\vec{d}_0 := \vec{d}/\|\vec{d}\|$, $\vec{d} := \pi(r) - r$, and ψ is the angle between $\vec{\imath}$ and $\vec{d}$. We put $\vec{\imath}_{\mathrm{s}} := \vec{\imath} \times \vec{d}_0/|\sin\psi|$ and introduce the projection $\vec{\imath}_{\mathrm{f}} := \vec{\imath} - \vec{d}_0 \cos\psi$ of $\vec{\imath}$ onto the plane $P = \mathfrak{T}_{\pi(r)}(S)$ normal to $\vec{d}$, which is spanned by $\vec{\imath}_{\mathrm{s}}$ and $\vec{\imath}_{\mathrm{f}}$. Both $\vec{\imath}_{\mathrm{s}}, \vec{\imath}_{\mathrm{f}}$ and P are computable by the robot in its local reference frame.

Let a MDE be given and $s(t) := \pi[r(t)]$. The two rays constituting $p[r(t)] \setminus \{s(t)\}$ continuously evolve over time. One of these continuous branches $R(t)$ is picked by somehow selecting a ray at $t = 0$ and as t grows, picking the updated ray as the nominee that is closer to the current ray than the competitor. Let $\varphi(t) \in (-\pi, \pi]$ be the angle from $R(t)$ to $\vec{\imath}_{\mathrm{f}}(t)$, where positive angles in the tangent plane P are counted counterclockwise when looking from the side of $N = -\vec{d}_0$.

In mode $\mathfrak{M}$, the robot is driven by the rule

$$\vec{u} = \overline{u}_d \,\mathbf{sgn}\left\{\dot{d} + \chi[d - d_{\sim}(t)]\right\} \vec{\imath}_{\mathrm{s}} \times \vec{\imath} - \overline{u}_{\mathrm{s}} \,\mathbf{sgn}\,(\varphi)\, \vec{\imath}_{\mathrm{s}}. \quad (6.1)$$

The maps $d_{\sim}(\cdot), \chi(\cdot)$ are defined in Fig. 2(b,c); $\overline{u}_d$, $\overline{u}_{\mathrm{s}}$, v_d, σ_χ, μ are positive controller parameters and $\overline{u}_d^2 + \overline{u}_{\mathrm{s}}^2 = \overline{u}^2$.

Since the unit vectors $\vec{\imath}_{\mathrm{s}} \times \vec{\imath}, \vec{\imath}_{\mathrm{s}}$, and $\vec{\imath}$ are mutually perpendicular, the control (6.1) is feasible, i.e., meets the last two requirements from (2.2). Any method of assessing $\dot{d}$ is welcome; numerical differentiation is among them. (Methods to cope with intricacies possibly associated with noisy data are surveyed in, e.g., [23].) The solutions of the closed-loop system are meant in Filippov's sense [24]. Given an initial state, such a solution exists and does not blow up in a finite time since the control is bounded. Its uniqueness is a more delicate matter; so we shall address all 'Filippov's'solutions.

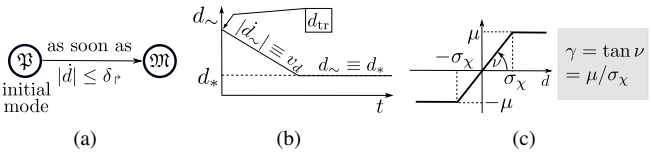

(a) (b) (c)

Fig. 2. (a) Switching logics; the functions (b) $d_{\sim}(\cdot)$ and (b) $\chi(\cdot)$.

VII. Main result

To solve the mission, it suffices to pick the parameters $\delta_{\uparrow}$, v_d, μ, σ_χ, $\overline{u}_d$, $\overline{u}_s$ of the controller so that

$$\mu_\delta := \mu + \delta_{\uparrow} < v, \qquad \sigma_\chi > 0, \quad (7.1)$$

$$\mu(\mu_\delta + v_d) + \overline{u}_N \left[v - \sqrt{v^2 - \mu_\delta^2}\right] < \Delta_c v^2, \quad (7.2)$$

$$\delta_{\uparrow} < \mu, \quad \delta_{\uparrow} < \gamma \min\{d_* - d_-; d_+ - d_*; \Delta_{\mathrm{in}}^d\}, \quad (7.3)$$

$$\overline{u}_d := \overline{u}_N, \quad \overline{u}_s := \overline{u}_{\mathfrak{T}}. \quad (7.4)$$

Here v, Δ_c and $\overline{u}_N, \overline{u}_{\mathfrak{T}}$ are taken from (2.2), (4.4) and Asm. 4.3, respectively, γ is defined in Fig. 2(b), and Δ_{in}^d is the distance margin between the circle C_{in} from Asm. 4.5 and the boundary of the operational zone (4.3):

$$\Delta_{\mathrm{in}}^d := \min\left\{\min_{p \in C_{\mathrm{in}}} \mathbf{d}_S[p] - d_-; d_+ - \max_{p \in C_{\mathrm{in}}} \mathbf{d}_S[p]\right\} \overset{\text{(a)}}{>} 0,$$

where $\mathbf{d}_S[p]$ is defined in (1.1) and (a) is due to Asm. 4.5. Also, it suffices to subject the exactness of the employed MDE to the following requirement

$$\beta < \arcsin \frac{\Delta_\varkappa \sqrt{\Delta_\tau}}{(1 + L_N d_*)\sqrt{2L_N}}, \quad (7.5)$$

where $\Delta_\tau, \Delta_\varkappa, L_N$ are taken from (3.2), (4.4), (4.5), respectively, and $\frac{\Delta_\varkappa \sqrt{\Delta_\tau}}{(1+L_N d_*)\sqrt{2L_N}} \le 1$, as can be shown.

These choices are feasible: (7.1) and (7.2) can be met by picking $\mu, \delta_{\uparrow}, v_d$ small enough, whereas $\sigma_\chi > 0$ is chosen arbitrarily. Then (7.3) can be met by reducing $\delta_{\uparrow}$, if necessary; (7.5) is feasible by Prop. 5.1. These give a guideline to experimentally tuning the controller. If a priory knowledge about the tunnel enables estimates of the involved tunnel's parameters, (7.1)—(7.5) can be used for analytical tuning.

Now we are in a position to state the main result.

Theorem 7.1: Let the tunnel be regular, relations (7.1)—(7.5) and Assumptions 4.2—4.5 hold, and let the robot be driven by the control law from Section VI.

Then the robot is not aligned with the direction to the surface in mode $\mathfrak{M}$ and solves the tunnel.

The first claim ensures that the controller is well-defined.

VIII. Simulation Tests

The numerical values of the basic parameters used in the tests are as follows: $v = 1\,m/s$, $\overline{u} = 1.65\,rad/s$, $d_* = 0.3m$, $v_d = 0.1m/s$, $\mu = 0.1m/s$, $\sigma_\chi = 0.005m$, $\delta_{\uparrow} = 0.02m/s$, $\overline{u}_d = 1.485rad/s$, $\overline{u}_s = 0.719rad/s$, $\alpha_e = 0.5rad$, $\vec{n}_{\mathrm{in}} = (0,1,0)$,

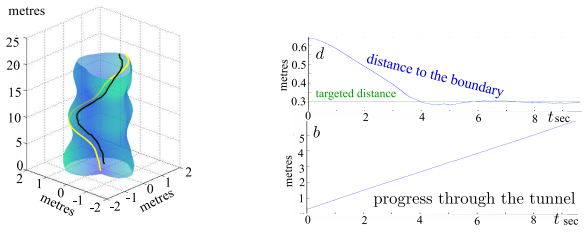

(a) (b)

Fig. 3. Passing through a deformed cylinder

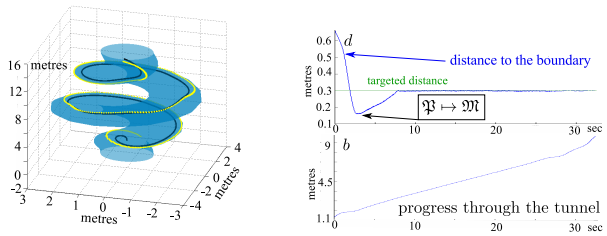

(a) (b)

Fig. 4. Passing through a spiral-like tunnel

$\tau = 0.01s$, where τ is the control update period. MDPBE from Sect. V was used as MDE. The distance measurement d was corrupted by an additive white Gaussian noise with the standard deviation $5mm$. The simplest numerical differentiation of the noisy data was used $\dot{d}(t) \approx \frac{d(t)-d(t-\tau)}{\tau}$. In practical setting, the robot often cannot continuously shift the direction of the ray along which the distance to the tunnel boundary S is evaluated. So we assume discrete shifts with angular increments, which induce leapwise displacements of the points where the beam hits S with a step of $\approx 1.6cm$.

In Figs. 3 and 4, the boundary surface S of the tunnel is shown in light blue, the paths of the robot and its projection onto S are depicted as black and yellow curves, respectively.

Figs. 3 deals with a quite deformed and vertically oriented cylinder, "progress" through which is assessed by the vertical coordinate. By Fig. 3(b), the robot successfully progresses through the tunnel since the very beginning at a nearly constant speed of $\approx 0.5m/s$. The targeted value $0.3m$ of the distance to S is reached for $\approx 6s$ and then is maintained with an accuracy of $\approx 1cm$, which looks like a fair price for the above measurement errors due to noises and imperfect ray focusing. A quite curvy robot's path in Fig. 3(a) is consonant with a somewhat complex geometry of the surface S, whose local patches (observed by the robot) give no solid clues about the best (i.e., vertical) direction of motion.

Fig. 4 deals with a spiral-like tunnel that is obtained by dragging a unit circle over the spiral with the parametric representation $x(s) = 2\cos(s), y(s) = 2\sin(s), z(s) = 5s/(2\pi)\ s \in [0, 6\pi]$. This tunnel whirls up around the vertical axis and so "progression" through it can be assessed in terms of the vertical coordinate. By Fig. 4(b), the distance d to S overshoots the desired value d_* during the preliminary mode $\mathfrak{P}$. In the main mode $\mathfrak{M}$, this distance monotonically converges to d_* for $\approx 8s$ and then stays near this value with nearly the same precision as in the previous test. Similarly, the robot progresses through the tunnel since the very beginning and at a nearly constant speed.

REFERENCES

[1] B. Bingham, et.al., "Robotic tools for deep water archaeology: Surveying an ancient shipwreck with an autonomous underwater vehicle," *J. of Field Robotics*, vol. 27, no. 6, pp. 702–717, 2010.

[2] A. Bachrach, R. He, and N. Roy, "Autonomous flight in unknown indoor environments," *International Journal of Micro Air Vehicles*, vol. 1, no. 4, pp. 217–228, 2009.

[3] C. White, D. Hiranandani, C. Olstad, K. Buhagiar, T. Gambin, and C. Clark, "The Malta cistern mapping project: Underwater robot mapping and localization within ancient tunnel systems," *J. Field Robotics*, vol. 27, pp. 399–411, 2010.

[4] N. Fairfield, G. Kantor, D. Jonak, and D. Wettergreen, "Autonomous exploration and mapping of flooded sinkholes," *Int. Journal of Robotics Research*, vol. 29, no. 6, pp. 748–774, 2010.

[5] A. Mallios, P. Ridao, D. Ribas, and M. Carreras, "Toward autonomous exploration in confined underwater environments," *J. of Field Robotics*, vol. 33, no. 7, pp. 994–1012, 2016.

[6] J. Mirats Tur and W. Garthwaite, "Robotic devices for water main in-pipe inspection: A survey," *J. of Field Robotics*, vol. 27, no. 4, pp. 491–508, 2010.

[7] A. Gargade, D. Tambuskar, and G. Thokal, "Modeling and analysis of pipe inspection robot," *Int. Journal of Emerging Technology and Advanced Engineering*, vol. 3, no. 5, pp. 120–126, 2013.

[8] A. Nayak and S. Pradhan, "Design of a new in-pipe inspection robot," *Procedia Engineering*, vol. 97, pp. 2081–2091, 2014.

[9] N. Fairfield, D. Jonak, G. Kantor, and D. Wettergreen, "Experiments in navigation and mapping with a hovering AUV," in *Springer Tracts in Advanced Robotics: Field and Service Robotics*, C. Laugier and R. Siegwart, Eds. Berlin: Springer, 2008, vol. 42, pp. 115–124.

[10] F. Kendoul, "Survey of advances in guidance, navigation, and control of unmanned rotorcraft systems," *Journal of Field Robotics*, vol. 29, no. 2, pp. 315–378, 2012.

[11] G. Lee, F. Fraundorfer, and M. Pollefeys, "MAV visual SLAM with plane constraint," in *Proc. of the IEEE International Conference on Robotics and Automation*, Shanghai, China, 2011, pp. 3139–3144.

[12] J. Courbon, Y. Mezouar, N. Guenard, and P. Martinet, "Visual navigation of a quadrotor aerial vehicle," in *Proc. of the Int. Conference on Intelligent Robots and Systems*, St. Louis, MO, 2009, pp. 5315–5320.

[13] M. Schwager, B. Julian, and D. Rus, "Optimal coverage for multiple hovering robots with downward facing cameras," in *Proc. IEEE Int. Conf. on Robotics and Automation*, Kobe, Japan, 2009, pp. 4016–4023.

[14] S. Grzonka, G. Grisetti, and W. Burgard, "A fully autonomous indoor quadrotor," *IEEE Trans. Rob.*, vol. 28, no. 1, pp. 90–100, 2012.

[15] A. Matveev, M. Hoy, and A. Savkin, "3D environmental extremum seeking navigation of a nonholonomic mobile robot," *Automatica*, vol. 50, no. 7, pp. 1802–1815, 2014.

[16] A. Matveev, H. Teimoori, and A. Savkin, "A method for guidance and control of an autonomous vehicle in problems of border patrolling and obstacle avoidance," *Automatica*, vol. 47, pp. 515–524, 2011.

[17] A. Matveev, M. Hoy, and A. Savkin, "The problem of boundary following by a unicycle-like robot with rigidly mounted sensors," *Robotics and Autonomous Systems*, vol. 61, no. 3, pp. 312–327, 2013.

[18] M. Hoy, A. Matveev, and A. Savkin, "Algorithms for collision-free navigation of mobile robots in complex cluttered environments: a survey," *Robotica*, vol. 33, no. 3, pp. 463–497, 2015.

[19] A. Matveev, A. Savkin, M. Hoy, and C. Wang, *Safe Robot Navigation Among Moving and Steady Obstacles*. Oxford, UK: Elsevier, 2016.

[20] A. Matveev, K. Ovchinnikov, and A. Savkin, "A method of reactive 3D navigation for a tight surface scan by a nonholonomic mobile robot," *Automatica*, vol. 75, pp. 119–126, 2017.

[21] W. Klingenberg, "Riemannian geometry," in *de Gruyter Studies in Mathematics*. Berlin: W. de Gruyter & Co., 1982.

[22] I. Shafarevich, *Basic Algebraic Geometry*, 2nd ed. Berlin: Springer-Verlag, 1994, vol. 1.

[23] "Advances in automatic differentiation," in *Lecture Notes in Computational Science and Engineering*, C. Bischof, H. Bücker, P. Hovland, U. Naumann, and J. Utke, Eds. Berlin: Springer-Verlag, 2008, vol. 64.

[24] A. Filippov, *Differential Equations with Discontinuous Righthand Sides*. Dordrecht, the Netherlands: Kluwer Academic Publishers, 1988.